THE SLAC NLC EXTRACTION & DIAGNOSTIC LINE*

J. Spencer, J. Irwin, D. Walz and M. Woods
Stanford Linear Accelerator Center, Stanford University, Stanford, CA 94309 USA

Abstract

A prototype extraction line for the Next Linear Collider is discussed that has several important functions that include optimizing luminosity, characterizing beam properties at the Interaction Point and transporting beams from the IP to a dump. Beam characterization includes measurements of current, position, profile, energy, polarization and low-order correlations on a bunch-to-bunch basis for feedback and stabilization. Prototype optical and diagnostic layouts are described that provide such functions. We also consider possibilities for e, μ and γ secondary beam lines and dump experiments as well as energy recovery and local reuse of an assumed 10MW in each 500 GeV beam.

I. Introduction

Our overall goal is to optimize the luminosity. While an important objective is to get the beams into their respective dumps with minimal detector backgrounds, it is also important to provide any monitoring and feedback that can optimize the usable collision rate at the IP. To accomplish this, we need to know the detailed composition and characteristics of the outgoing disrupted beams. These beams have a significant number of pairs and more photons than leptons. Based on a 'worst' case prediction for these beams we then describe how we arrive at our 'final' result.

Due to the high power in the outgoing photon beam and the cost of beam dumps we decided that the photons and leptons should share a common dump. This implies an available distance for beam studies of 150 m. Because the SLC was a prototype for the NLC we begin by reviewing the SLC and FFTB experience relative to the NLC design.

II. Comparison with SLC

One advantage for the NLC relative to SLC is a horizontal crossing angle ($\theta_{c,x}\approx 2\times 10$ mrad) at the IP that allows us to avoid kickers and septa for separating the counterpropagating beams. This enables us to reverse polarities between the ingoing and outgoing quadrupoles for better control of the larger horizontal disruption angles.

Rather than 30 kW in each SLC beam one has to deal with nearly 10 MW in each NLC beam. There is a factor of ten in energy i.e. 500 GeV beams for the NLC, the same RF pulse repetition rate of 120/s and a factor of twenty or so in beam current per RF pulse from accelerating a multibunch train in each pulse. This increased beam power poses certain problems for intercepting detectors and implies significantly higher operating costs. For 10¢/kWh, this represents a potential refund of as much as \$45K/day if energy is restored to the grid or otherwise recycled.

*Supported under Dept. of Energy contract DE-AC03-76SF00515.

The lower invariant emittances and the factor of ten in energy result in significantly greater disruption effects in the NLC that permit most of the SLC measurements and others that aren't practical there. However, because the disruption angle is dominated by energy, we can measure the energy loss distribution and use precise RF BPMs in the beginning of the line to measure position, angle and timing of individual bunches. This is impractical for SLC e.g. Σ_y=1 μm and N=3.5·10^{10} produces a peak deflection angle that is more than double our worst case.

III. Basic Design Procedures and Constraints

The optics can only be realized in practice after we know the characteristics of the outgoing beam. The procedure was to take the upstream final focus design in the form of TRANSPORT[1] and convert this to DIMAD[2] for predicting the spot characteristics at the IP due to emittance growth from synchrotron radiation in the dipoles and quadrupoles. One assumption here was that the energy loss, especially in the quads, can be neglected. The predicted beam parameters resulting from DIMAD were then used in ABEL91[3] to predict the composition and characteristics of the outgoing beam as well as to produce ray sets for all particle types for analysis and tracking. The ABEL calculations were compared to analytic calculations before being used to simulate the dump line with TRANSPORT (for design) and TURTLE (for tracking)[4].

The available length of the dump line was set by the outgoing photons and the assumed size of the dump:

$$12\sigma_{x'}^{\gamma} \times L_D \leq 2R_D$$

where L_D is the distance from the IP to the dump face and R_D is its radius. For a dump window of 20 cm in diameter and outgoing angular spreads of $\sigma_{x',y'}$=92,43 μrad from ABEL, we have 150 m of space available for beam studies.

The design procedure was complicated by the different species of outgoing particles that had to pass without intercepting *anything* as well as by the comparatively large angular and energy spreads induced by the beam-beam interaction. Besides constraining our design options this forced us to continually constrain the magnet apertures and lengths to insure reasonable magnets. Other constraints were imposed by the measurements and experiments that might be required. For example, electron spin rotation and depolarization constrained the strength and disposition of the dipoles. A related constraint was the need to capture off energy bunches or ones that did not collide and lose energy. The latter includes those resulting from beam-beam deflection scans. Other constraints will be discussed in the relevant sections.

IV. Optics

Once the disrupted electrons have cleared the detector, taken to be $\pm$5 m along the IP, using essentially a quadrupole doublet,

we observe where the disrupted beam crosses the photon beam using third order TURTLE. Because this was nearly 20 m from the IP and it took 10 m to get the full energy beam moving parallel toward the dump, we find the first available space for diagnostics between 11 and 16 meters. RF BPMs [5] are assumed to begin at 5 m where the outgoing beams are still small and C-Band cavities could have apertures comparable to the quads($\approx \lambda/4$).

The first dipole of a horizontal chicane, used to separate the outgoing photon and electron beams, begins at 16 m. It allows separate experiments, before recombining both beams into a common dump. Figure 1 shows the Twiss functions when the four bends are sized to separate the two beams by 12σ. Their maximum separation is

$$\Delta x = 2\rho_B(1 - cos\theta_B) + L_1 tan\theta_B$$

where θ_B is the bend angle for the full energy of any one rectangular dipole of length L_B=$\rho_B sin\theta_B$ and L_1 is the separation between bends BD1 and BD2. Notice that this is just the dispersion η_x in the center of the chicane. This separation requires a minimum distance of

$$L_{min} = 2\rho_B sin\theta_B + L_1 \ .$$

The change in the bunch separation, due to the chicane, after this point in the central region is

$$R_{56} = \frac{\delta l_z}{\delta p/p} = 2\rho_B(tan\theta_B - \theta_B) + L_1 tan^2\theta_B \ .$$

This is proportional to the RF phase shift[6]. Thus we have a common beam pipe and sufficient dispersion to measure the energy and spread of the undisrupted beam.

For example, if we want to use the first bend for analyzing low energy particles from the IP or from a laser interaction before this bend, then the first order resolving power for some downstream location L is

$$R_1(\rho, \theta, L) = \frac{\rho(1 - cos\theta) + L \cdot tan\theta}{[x_i cos\theta + x_i'(\rho sin\theta + L/cos\theta)]} \ .$$

In the middle of the chicane R depends on the optics we impose. $R_{12}\rightarrow 0$ for point-to-point so R=$\Delta x/(10\sigma_x^*$=8000 for a magnification of 10 i.e. this region of the chicane can resolve a single beam, undisrupted energy spread of δp/p=0.0125% while the region directly in front of BD2 gives $R\approx$800 or 0.13% capability.

Notice that there were several factors that constrained the bends e.g. electron spin rotation as well as the energy resolution necessary to resolve low-energy electrons near the Compton edge (required for monitoring beam polarization). Further, dipoles drive many higher order aberrations that act to blow the beam up that require higher multipoles to correct. These were not needed to get the beams into the dump with the 12σ constraint through the line.

V. Instrumentation

The guiding principle in the instrument layout Fig. 2 was to minimize the material in the high power beams. Thus, there is a significant use of lasers to control the production of additional particles. Nevertheless, since beamstrahlung is unavoidable, there are possibilities[7] to use either Compton or beamstrahlung photons that could prove quite useful for monitoring

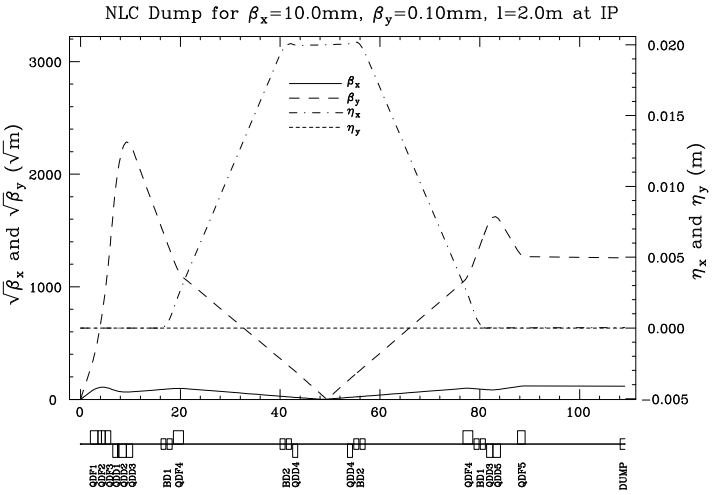

Figure. 1. Prototype Optical Layout for the NLC Dump Line.

the position, size and correlations of the bunches at the IP on a bunch-to-bunch basis. Clearly, beamstrahlung is quite sensitive to any changes in these parameters at the IP. In fact, the photon distribution is a better measure of the bunch profile at the IP than the outgoing, disrupted electrons. We also assume wire scanners and screens similar to SLC[8].

An important tool for optimizing luminosity at the SLC is the beam-beam deflection scan[9]. This gives the deflection of each beam as a function of the relative offset. Typically, this procedure requires many points and makes a number of assumptions about the beam's characteristics. Multi-bunch trains complicate this. Depending on the beam's aspect ratios, one can estimate many effects as though an additional quad was added e.g. energy loss can be calculated. In lowest order this is proportional to the beam sizes but is very small for SLC so that it is masked by the incident beam's energy spread. Taking the simple expression for the deflection of one particle at the periphery of the other beam:

$$\theta_D \approx p_\perp/p = \frac{2Nr_e}{\gamma\sigma_\perp} \rightarrow \frac{2Nr_e}{\gamma(\sigma_x + \sigma_y)} = \frac{D_{x,y}\sigma_{x,y}}{\sigma_z} \ ,$$

we find a maximum outgoing angle of $\theta_{x,max}$=θ_D=256 μrad. The disruption parameters are $D_{x,y}$=0.104,10.2 while $\sigma^*_{x,y}$=245,2.5 nm. D_y is so large that there is over focusing or a thick lens effect whereas the focusing over the length of the beam in x is weaker but cumulative i.e. more like a simple thin lens. This is most easily dealt with by reversing the polarity of the first outgoing quad.

The final angle of relevance here is the spin precession angle θ_s. This can be expressed in terms of the spin tune:

$$\nu_s \ = \ \frac{E[GeV]}{0.44065} \cdot \frac{\Theta}{2\pi} \ ,$$

where Θ is some deflection angle in radians. For the bends used here this is typically 2-4 times the maximum disruption angle θ_D=256 μrad. The effective polarization after such a bend is $P_{eff} = P_{inc}cos(2\pi\nu_s)$=0.42-0.84 although this is just a rotation in the bend plane.

We need to make a good measurement of the polarization that doesn't interfere with the primary disrupted beam on its way to

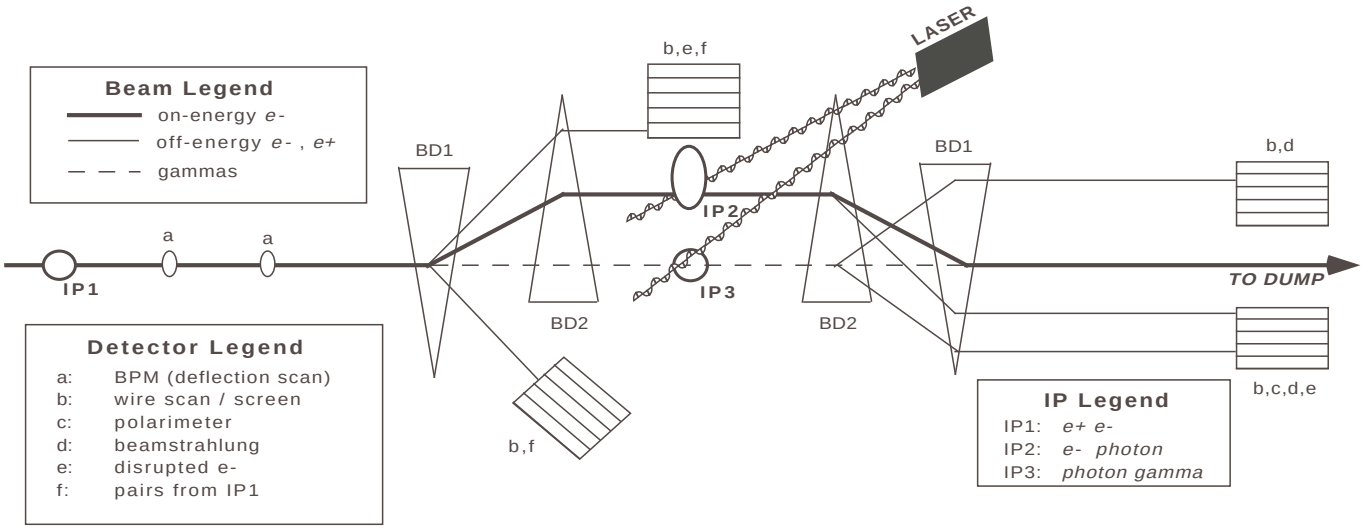

Fig 2: NLC Electron Extraction & Diagnostic Line

the dump or other measurements. While this can be done at other locations, it is done here in the middle of the chicane shown in Fig. 2 because this is where the dispersion is largest and the net rotation from the bends is zero. In our worst case scenario 20% of the beam goes undisrupted i.e. should have its original polarization. Compton scattering can then be used to monitor the polarization at this point by measuring the asymmetry in the scattered electrons as a function of laser polarization[10].

For best results, one needs to measure the electrons near the Compton edge with good resolution. In lowest order:

$$\epsilon_c^{edge} = \frac{\epsilon_{in}}{1+x} = \frac{\epsilon_{in}}{1+0.0153\epsilon_{in}(GeV)\omega_L(eV)} \approx 26 \text{ GeV}.$$

Because these electrons fall on the far tail of the disrupted beam spectrum, the only requirement is the ability to resolve their energy to one-half GeV i.e. a resolving power of only R=P/ΔP $\geq$ 50. Because R=8000 for the full energy beam, there is clearly no problem i.e. the laser spot can be any required size up to $\eta\delta\approx$4 mm. This is also a good place to measure the electron beam profile and disruption characteristics to monitor bunch overlap, synchronization and luminosity.

VI. The Beam Dump

The dump has to dispose of essentially all of the power. Water is the primary absorber in a cylindrical vessel housing a vortex-like flow of water with vortex velocity ≈1-1.5 m/s normal to the beam momentum. The vessel is 1.5 m diameter and has a 5.5-6.5 m long water section, followed by ≈ 1 m of water-cooled solids to attenuate a 500-750 GeV EM cascade shower. The beam enters through a thin window ≈1 mm thick and 20cm diameter. Production of ≈3 l H_2/10 MW beam power from radiolysis[11] can be mitigated with a catalytic H_2/O_2 recombiner that has a closed loop system that contains all radioisotopes.

References

[1] K.L. Brown et al., TRANSPORT, SLAC Report 91, May 1977.

[2] R.V.Servranckx, User' Guide to DIMAD, July 1993.

[3] K. Yokoya, ABEL, A Computer Code for the Beam-Beam Interaction in Linear Colliders, NIM **B251**(1986)1 and Toshiaki Tauchi et al. Part. Accel. **41**(1993)29. We thank Mike Ronan for help in getting the latest version of ABEL (Analysis of Beam-beam Effects in Linear colliders) running on VM system.

[4] D.C. Carey et al., DECAY TURTLE, SLAC Report 246, March 1982.

[5] S. Hartman and N. Shintake, private communication.

[6] For energy recovery we want the dispersion and the angular dispersion to be zero to all orders in δ, x' and y' because of the beam-beam interaction. This implies a high order achromat that was not otherwise required.

[7] J. Norem, et al., Tests of a High Resolution Beam Profile Monitor, These Proceedings.

[8] Clive Field, NIM, To Be Published.

[9] P. Bambade, et al., Observation of Beam-Beam Deflections at the SLC, Phys. Rev. Lett. **62**(1989)2949.

[10] M. Woods, Polarization at SLAC, SLAC-PUB-6694, October 1994.

[11] D.R. Walz et al., Radiolysis and H Evolution in the A-Beam Dump Radioactive Water System, SLAC-TN-67-29, October 1967.